



Published in final edited form as:

*Biochemistry*. 2010 February 16; 49(6): 1207. doi:10.1021/bi9017208.

## Decoding of lipoprotein – receptor interactions; Properties of ligand binding modules governing interactions with ApoE

Miklos Guttman, J. Helena Prieto, Johnny E. Croy, and Elizabeth A. Komives\*

Department of Chemistry and Biochemistry, University of California, San Diego, 9500 Gilman, Dr. La Jolla, CA 92093-0378

### Abstract

Clusters of complement-type ligand binding repeats in the LDL receptor family are thought to mediate the interactions between these receptors and their various ligands. Apolipoprotein E, a key ligand for cholesterol homeostasis, has been shown to interact with LDLR, LRP and VLDLR, through these clusters. LDLR and VLDLR each contain a single ligand-binding repeat cluster, whereas LRP contains three large clusters of ligand binding repeats, each with ligand binding functions. We show that within sLRP3, the three-repeat subcluster CR16-18 recapitulated ligand binding to the isolated receptor binding portion of ApoE (residues 130-149). Binding experiments with LA3-5 of LDLR and CR16-18 showed that a conserved W25/D30 pair appears critical for high affinity binding to ApoE(130-149). The triple repeat LA3-5 showed the expected interaction with ApoE(1-191)•DMPC, but surprisingly CR16-18 did not interact with this form of ApoE. To understand these differences in ApoE binding affinity, we introduced mutations of conserved residues from LA5 into CR18, and produced a CR16-18 variant capable of binding ApoE(1-191)•DMPC. This change cannot fully be accounted for by the interaction with the proposed ApoE receptor binding region, therefore we speculate that LA5 is recognizing a distinct epitope on ApoE that may only exists in the lipid bound form. The combination of avidity effects with this distinct recognition process likely governs the ApoE-LDL receptor interaction.

The low density lipoprotein (LDL) superfamily of receptors mediates cholesterol uptake into cells (1). Members of this family share many structural characteristics and sequence homology including an extracellular ligand binding domain consisting of complement-type repeats (CRs), also called ligand binding modules (LAs), epidermal growth factor precursor homology repeats (EGFs),  $\beta$ -propeller domains, and a single transmembrane segment with an intracellular domain (Fig. 1). The most well characterized of these receptors, LDLR, is genetically linked to hypercholesterolemia (2). LDLR family members recognize apolipoproteins on the surface of lipid particles, and Apolipoprotein E, in particular, plays an important role in receptor mediated cholesterol uptake (3). Although LDLR is the primary receptor for cholesterol carrying lipoproteins, studies have shown that the LDL receptor-related protein (LRP) and the very low density lipoprotein receptor (VLDL) also mediate the uptake of ApoE enriched  $\beta$ -VLDLs (4–7).

\*To whom correspondence should be addressed: ph: (858) 534-3058, FAX: (858) 534-6174, ekomives@ucsd.edu.

This supplemental material is available free of charge via the Internet at <http://pubs.acs.org>.

Supporting Information: Supporting information is provided with this manuscript that includes: additional surface plasmon resonance data supporting the binding of CR16-18 to ApoE(141-155)<sup>2</sup> (Suppl. Figure 1); HSQC spectra showing the shifts in amide resonances during NMR titration experiments of CR16, CR17, CR18, LA3, LA4, and LA5 with Ub-ApoE(130-149) (Suppl. Figure 2); HSQC spectra showing the shifts in amide resonances during NMR titration experiments of CR16-18 with Ub-ApoE(130-149) (Suppl. Figure 3); and HSQC spectra showing the shifts in amide resonances during NMR titration experiments of CR17, CR18, LA3, LA4, and LA5 with Ub-RAPD3 (Suppl. Figure 4).

LRP recognizes at least 30 different ligands which indicate the diversity of LRP's functions (8). The 600kDa precursor is processed by furin cleavage, and the two chains remain non-covalently bound at the cell surface (9). The receptor associated protein (RAP), serves as a chaperone assisting the maturation of LRP (10,11) and can interact with ligand binding clusters of this family of receptors, blocking the binding of certain ligands (12). Each of the three helical bundle domains of RAP can interact with receptors, but the third domain (RAPD3) has the highest affinity for these ligand binding clusters (13). A semi-conserved aspartate within these CRs was shown to be critical for RAP binding (14). The extracellular chain of LRP contains four clusters of CRs referred to as sLRPs (Fig. 1). Studies have shown that isolated sLRPs can interact with many ligands of LRP *in vitro* (15–18). Much like LDLR, LRP was shown to bind and internalize  $\beta$ -VLDLs, but only if the VLDLs were enriched with ApoE (4). Other distinctions between the two receptors have been observed including calcium dependence (19,20), and RAP inhibition of ligand binding (12,18).

Each CR/LA domain is composed of about 40 amino acids with a well conserved fold stabilized by three disulfide bonds, and a cluster of acidic residues that form a high affinity calcium binding site. Mutations at the calcium binding site wreck proper folding and are associated with familial hypercholesterolemia (21). Several CR domains have now been solved by both NMR and crystallographic methods (22), and show very little deviation in their overall fold. It is believed that high variability in short loops of these repeats results in different surface contours and electrostatics, which establish ligand specificity (1,23).

ApoE is a constituent of several lipoprotein particles, and common alleles have been associated with type III hyperlipoproteinemia (24). ApoE is composed of two domains that are both involved in lipid binding, but only the N-terminal domain is required for receptor binding (25). Several studies agree that the critical receptor recognition site is within residues 140-150 (26–28). Chimeric lipoproteins in which this segment is spliced into an unrelated lipoprotein have found that substitution with residues 131-151 of ApoE is enough for receptor recognition (29). Peptides from this region of ApoE incorporated into lipoprotein particles, enhanced uptake both *in vitro* and *in vivo* (30,31). Binding studies with ApoE(130-149) and ApoE(140-151)<sup>2</sup> have shown that both can directly interact with the three complete sLRPs (2, 3, and 4) of LRP (32).

The structure of the N-terminal domain of ApoE has been solved (33), and although residues 131-151 form a surface-accessible helix in the structure, the N-terminal domain alone cannot bind LDL receptors with high affinity. Low resolution structural information indicates that the ApoE helical bundle adopts a new conformation when it is present in lipoprotein particles (34–36). One hypothesis is that when embedded in lipoproteins, ApoE residues 140-150 are in a different conformation for high affinity receptor binding than that observed in the crystal structure of the N-terminal domain alone (37). In addition, upon lipid binding, the region downstream of the 140–150 site, which also contains critical residues for receptor binding, becomes structured (24,38–40). Thus, it is also possible that this downstream region forms a high affinity receptor recognition site in the lipid bound state of ApoE.

Studies aimed at narrowing down the exact binding modules involved in recognizing ApoE have found minimal units in LDLR (41,42) and VLDLR (43), but similar studies on LRP have not yet been performed. Deletion studies in LDLR have implicated LA5 as the critical repeat for  $\beta$ -VLDL binding (42). LA45 was shown to be the minimal unit of LDLR capable of binding ApoE(1-191)•dimyristoyl-phosphatidylcholine (DMPC) particles *in vitro*, which mimic the lipid bound conformer of ApoE (41). Similar studies have implicated repeats 5 and 6 (VLA56) of VLDLR in ApoE binding (43). Interestingly both LA45 and VLA56 have a uniquely long linker sequence connecting the two repeats. Based on these data we performed sequence alignments in order to discover possible ApoE-binding sites in LRP. We present results from

binding experiments on a three-CR repeat fragment of LRP, and comparisons of its binding with combinations of repeats from LDLR. Together, the results reveal specific regions within LDLRs that govern the mechanism by which they recognize ApoE containing lipoproteins.

## Materials and Methods

### Sequence alignments

Sequence alignments were performed to search for the three-CR repeat sequences that would most likely bind to ApoE based on the fact that within LDLR, the three-repeat segment LA3-5 contains the ApoE binding site. The LA3-5 sequence (Uniprot # P01130) (residues: 84-214, numbering referring to the mature protein) without the additional linker between LA4 and LA5 (residues: 167-172) was used to search for homology within each sLRP (Uniprot # Q07954), using sequence alignment with LALIGN software (Bill Pearson, University of Virginia, Charlottesville) with the BLOSUM35 matrix with default values entered for gap penalty. The regions that contained the highest homology in each sLRP were CR3-5 (831-956), CR16-18 (2712-2838) and CR25-27 (3471-3516) (numbering according to mature LRP-1). To further analyze the sequences for unique residues that might be involved in ApoE binding, alignments of LA45 from LDLR and VLA56 from VLDLR from various species were made with genedoc 2.6 (44) (uniprot accession numbers: P01130, P98155, P35951, P98156, P35952, P98166, Q28832, P35950, Q99087, Q6NS01, Q99088, O77505, P20063, P35953, P98165, Q7ZZT0, Q6S4M2).

### Protein expression and purification

Smaller subdomains of LRP; CR3-5, CR16-18 and CR25-27 were cloned into the pPIC9K as described previously for thrombomodulin (45). CR16 (2712-2754), CR17 (2751-2798) CR18 (2794-2838), and multiple repeats CR1617, CR1718, and CR16-18 of human LRP, and residues 88-126 (LA3), 123-167 (LA4), 171-214 (LA5), 123-214 (LA4-5) and 88-235 (LA3-5) of the human LDLR (numbering for mature forms) were amplified by PCR and cloned into the pMMHb vector (46) modified to include an additional thrombin cleavage site after the TrpLE peptide. DNA oligonucleotides were inserted at the 3' BamH1 site to yield a C-terminal FLAG-tag. All mutants were made using either inverse PCR (47) or Quickchange (Stratagene, La Jolla, CA, USA) mutagenesis, and verified by DNA sequencing. CR17<sup>3</sup> was constructed by inserting CR17 with identical sticky ends into the BamH1 site of CR17 in the pMMHb vector, and screening for multiple insertions with correct orientation. Inverse PCR mutagenesis was used to remove CR17 from CR16-18 yielding a two repeat CR16( $\Delta$ 17)18. A  $\beta$ 2-swap mutation was made in CR18 in which residues 186-193 of LA5 were substituted into CR18 at positions 2809–2816. An expression vector for His tagged ApoE 1-191 was a kind gift from S. Blacklow. A Ubiquitin (Ub) fusion vector was generated by cloning the DNA sequence for human Ubiquitin into the Nco1 and BamH1 sites of vector pHis8 (48). RAPD3 (218-323), and ApoE(130-149) were inserted at the 3' end of this Ubiquitin (Ub) fusion vector to generate Ub-RAPD3 and Ub-ApoE(130-149). ApoE(130-149) and ApoE(141-155)<sup>2</sup> were synthesized with N-terminal biotinylation on a 9050 peptide synthesizer (Applied Biosystems, Foster City, CA, USA). A scrambled ApoE(130-149) was also synthesized with the sequence LREKKLRVSALRTHRLELRL. Purification of GST-RAP has been described previously (18). His tagged ApoE(1-191) was expressed in BL21-DE3, purified and complexed with dimyristoyl-phosphatidylcholine (DMPC) (Avanti Polar Lipids, Alabaster, AL, USA) as described previously (41). Ub-ApoE(130-149) was expressed and purified as described for Ub-RAPD3, with an additional cation exchange step prior to gel filtration to remove degradation products.

LRP sLRPs were expressed in *P. pastoris* as described previously (18). Each CR fragment was expressed in *E. coli* strain BL21-DE3 cells. Cultures were grown in M9 minimal media

supplemented with NZ amine at 37°C to OD<sub>600</sub> 1.0 and induced with 0.5mM IPTG. Isotopic labeling was achieved using M9 minimal media with <sup>15</sup>NH<sub>4</sub>Cl (1g/L) and <sup>13</sup>C glucose (3g/L) (Cambridge Isotope Labs, Andover, MA, USA). After 12 hrs of expression, cells were harvested and lysed by sonication. Inclusion bodies were isolated by centrifugation and resuspended in resolubilizing buffer (8M Urea, 50mM Tris (pH 8.0), 150mM NaCl, 1mM β-mercaptoethanol). Proteins were captured with Ni-NTA (Qiagen, Hilden, Germany) and washed with a gradient (50 ml to 50 ml) of resolubilizing buffer to refolding buffer (50mM Tris (pH 8.2), 400mM NaCl, 10mM CaCl<sub>2</sub> and 1.5mM/0.4mM reduced/oxidized glutathione). Columns were sealed and the resin was allowed to mix continuously by rocking in refolding buffer at 4°C for three days after which they were washed with 50mM Tris (pH 8.0), 150mM NaCl, 10mM CaCl<sub>2</sub> and treated with active bovine thrombin (40μg/L expressed protein) for 12 hrs at 25°C. Refolded, cleaved CRs were then purified by C18 reverse phase HPLC (Waters, Milford, MA, USA). Constructs containing LA4 needed an additional purification step to resolve disulfide isomers (Guttman et al., submitted). The purified CR repeats(s) were lyophilized from the HPLC buffer and stored at -80°C. All expressed proteins were analyzed by MALDI-TOF on a Voyager DE-STR (Applied Biosystems, Foster City, CA, USA) with sinnapinic acid (Agilent, Santa Clara, CA, USA) as the matrix.

### **Biacore**

SPR experiments were performed on a Biacore3000 with 300 RUs of biotinylated apoE (130-149) or apoE(141-155)<sup>2</sup> immobilized onto the chip (32). Binding sensograms were collected for a series of sLRP subdomains ranging in concentration from 62.5nM to 16μM at 5μL/min. The surface was regenerated between injections by a two minute injection of 1M NaCl. Each series of injections were fit globally to a 1:1 binding model with a drifting baseline using BiaEvaluation v 3.1.

### **ITC**

Calcium binding to various CR- and LA-repeats was assessed by titrations monitored with a MicroCal VP-ITC calorimeter. Lyophilized protein was resuspended in 20mM Hepes (pH 7.4), 150mM NaCl, 0.02% azide, that was treated with Chelex (Biorad, Hercules, CA, USA). Complement repeats were titrated with 10 fold molar excess of CaCl<sub>2</sub> in the same buffer at 35°C. Binding isotherms were fit to single binding site models in Origin 6.0, except CR16-18 which was fit to a two site binding model (OriginLab, Northampton, MA, USA).

### **ApoE (130-149) Pulldowns**

All reactions were carried out in HBST (20mM Hepes pH 7.4, 150mM NaCl 0.02% sodium azide, 0.1% Tween-20 (Biorad, Hercules, CA, USA) containing either 2mM CaCl<sub>2</sub> or 2mM EDTA. ApoE peptide (130-149) with an N-terminal biotin was immobilized onto streptavidin agarose (Fluka, Buchs, Switzerland) at saturating concentrations as described previously (32). Either uncoupled beads or scrambled ApoE(130-149) peptide was used as a negative control. FLAG-tagged complement repeat constructs were added (500nM), reactions were left rocking at 25°C for 2 hours, then washed twice with the same buffer, resolved by SDS-PAGE, probed with anti-FLAG antibody (a generous gift from P. van der Geer) and detected by chemiluminescence (Western Lightening Plus kit, Perkin Elmer, Waltham, MA, USA). GST-RAP (6μM) and high molecular weight (HMW) heparin (5mg/mL) (Sigma-Aldrich, ST. Louis, MO, USA) were tested as inhibitors. For comparisons of CR16-18, CR1617, CR1718, and CR16(Δ17)18, 500nM and 5μM concentrations were used in similar pulldown binding assays.

### **GST-RAP and ApoE-DMPC pulldowns**

GST-RAP (1μM) or ApoE(1-191)•DMPC (2μM) was mixed with various FLAG-tagged LA/CR constructs (1μM), at 25°C for 1 hour, in HBST with either 1mM calcium or 1mM EDTA.

In order to avoid the high background caused by minor precipitation of ApoE-DMPC, reactions were centrifuged for 5 minutes after the incubation step, and the supernatant was added to anti-FLAG agarose (Sigma-Aldrich, ST. Louis, MO, USA) for 30 minutes. Pulldowns were washed 3 times in binding buffer, resolved by SDS-PAGE and probed by western blot with antibodies anti-ApoE (Millipore, Billerica, MA, USA), anti-GST (GE healthcare, Uppsala, Sweden) and anti-FLAG rabbit serum. RAP competition was performed with addition of 6 $\mu$ M (3 fold excess) of GST-RAP.

## NMR

NMR spectra were collected on a Bruker Avance 800 MHz, or a Bruker Avance III 600 MHz spectrometer equipped with a cryoprobe at 307°K.  $^{15}\text{N}$ ,  $^{13}\text{C}$  labeled CR16-18 (0.5mM) was resuspended in 20mM Hepes (pH 6.6), 150mM NaCl, 5mM  $\text{CaCl}_2$ , 50mM arginine, 50mM glutamic acid, 10%  $\text{D}_2\text{O}$  and 0.02% sodium azide. Amide assignments were made with  $^1\text{H}$ - $^{15}\text{N}$  HSQC, HNCO, HNCA, HN(CO)CA, HNCACB experiments. Assignments for CR17 were also made using a 0.7mM sample of  $^{15}\text{N}$ ,  $^{13}\text{C}$  labeled CR17 at pH 7.45 in the same buffer, with HSQC, CBCANH, CBCANNH experiments.  $^{15}\text{N}$  labeled CR16 (0.4mM) and CR18 (0.6mM) were titrated from pH 6.6 to pH 7.45 to monitor pH-dependent chemical shift changes and to transfer the assignments from CR16-18 at pH 6.6.  $^{15}\text{N}$   $^{13}\text{C}$  labeled LA45 was assigned with the same experiments and buffer conditions used for CR17, except without the 50mM Arg/Glu, and assignments were transferred to individual LA4 and LA5. The data were processed using Azara (Wayne Boucher and the Department of Biochemistry, University of Cambridge) and analyzed in Sparky (T. D. Goddard and D. G. Kneller, SPARKY 3, University of California, San Francisco). All assignment data for CR16-18, CR17 and LA45 have been deposited to the BMRB (IDs 16509, 16482 and 16480).

## NMR titrations

All titrations of CR/LA(s) with various ligands were performed in 20mM Hepes (pH 7.45), 150mM NaCl, 10mM  $\text{CaCl}_2$ , and 0.02% azide in 10%  $\text{D}_2\text{O}$  at 307°K. Due to self association of CR17, all CR concentrations were kept under 100 $\mu$ M, which became problematic at large excess of titrated ligands due to the appearance of peaks from natural abundance  $^{15}\text{N}$  from the ligand. Identical aliquots of  $^{15}\text{N}$  labeled CR/LAs were resuspended in either Ub-fused ligand or Ub, adjusted to pH 7.45, and mixed in various ratios to yield samples with varying concentrations of ligand but identical total protein concentration. Only well resolved peaks in all titrations were used for affinity calculations. Some residues exhibited slow exchange binding kinetics in the CR18-RAPD3 titrations, so only shifts showing fast exchange kinetics were analyzed. For some titrations the highest ligand concentration could not be included in the fit due to poor signal to noise and broadening of peaks.  $^{15}\text{N}$  shifts were normalized by a factor of 9.8, and the net shift for every cross peak in both  $^1\text{H}$  and  $^{15}\text{N}$  was calculated. A global fit of all perturbations (>0.015ppm) was implemented as described previously (49). Titration curves were also fit to measurements of the largest cross peak perturbation and the sum of all individual perturbations. Overall  $K_D$ s are reported as the average from these three methods, with the standard deviation of all measurements.

## Results

### Identification of an ApoE-binding subdomain in sLRP3

Alignments of each sLRP in LRP1 with LA3-5 in LDLR showed that CR3-5, CR16-18 and CR25-27 had the highest similarity to LA3-5. These subdomains were cloned and expressed in *P. pastoris* for surface plasmon resonance (SPR) analysis. Experiments to probe the binding of each sLRP subdomain to immobilized biotinylated ApoE(141-155)<sup>2</sup> and biotinylated ApoE (130-149) showed that of the three, only CR16-18 had binding affinities comparable to the full length sLRP ( $K_D$  ~200nM) (Supp. Fig. 1). SPR experiments also revealed that CR16-18

refolded from *E. coli* inclusion bodies bound as well as when purified from *P. pastoris*. Affinity pulldown assays verified that CR16-18 could bind immobilized ApoE(130-149) and that this interaction was calcium dependent and inhibited by heparin, and RAP (Fig. 2a). Pulldown assays of FLAG-tagged CR constructs also showed that two repeat constructs had significantly weaker affinity for ApoE(130-149), of which CR1718 bound the best (Fig. 2b). CR1718 also exhibited roughly ten-fold weaker binding as qualitatively assessed by SPR analysis.

### Refolding and calcium-binding of the LRP1 CR(s)

Refolded LRP1 CR(s) were titrated with calcium, and binding was monitored by isothermal titration calorimetry (ITC). Calcium affinities for CR16, CR17, and CR18, were  $0.72 \pm 0.04 \mu\text{M}$ ,  $7.5 \pm 2 \mu\text{M}$ , and  $13.7 \pm 0.7 \mu\text{M}$  respectively, which are similar to previously published values for CR/LA domains (50,51). Calcium titration of the three repeat CR16-18 showed two binding events, and the data were fit to a two-site binding model (Fig. 3a). Although the first site has relatively few data points, the thermodynamic parameters are consistent with CR16 binding initially with high affinity, followed by CR17 and CR18 binding with weaker affinity, but higher enthalpy. Mutation of D2778 to Ala in CR17 had no effect on calcium affinity ( $K_D$   $7.4 \pm 0.5 \mu\text{M}$ ). NMR  $^1\text{H}$ - $^{15}\text{N}$  HSQC spectra in the presence of calcium indicated that each repeat was well folded, both as the isolated domain and in the CR16-18 subdomain (Fig. 3b). Nearly all of the expected cross peaks were observed for CR16 and CR18, but a significant number (12 of 49) of cross peaks in CR17 were missing.

### Titration of ApoE(130-149) binding to LRP1 CR(s)

NMR titrations were used to examine the binding of CR16-18 to ApoE(130-149). Initial titration experiments with ApoE(130-149) peptide resulted in solubility problems, so ApoE(130-149) was expressed as a ubiquitin (Ub) fusion protein, and this alleviated the solubility problems even at concentrations above 1mM. Binding of Ub-ApoE(130-149) caused specific perturbations in each repeat (Supp. Fig. 2). The most notable perturbation was a strong downfield  $^1\text{H}$  shift for the indole of W2773 in CR17. The same was true for the indoles of W2732 in CR16, and W144 in LA4. F2816, which is in the same position in CR18, showed largest perturbation in this repeat. Other amides showing large perturbations included: K2730, W2732, D2735, G2736, S2737, A2746, in CR16; F2760, C2768, V2769, R2772, W2773, D2776, A2790, in CR17; and R2809, C2818, D2829, E2833, in CR18; W144, D147, D149, and D151 in LA4; and S172, W173, and G178 in LA5. Titrations of Ub-ApoE(130-149) with individual CRs showed identical shifts to those observed in CR16-18 (Supp. Fig. 3). Plots of relative perturbations in each show the majority of large shifts are located in two loops between the third and fifth cysteines (residues 23-32 according to consensus numbering in Fig. 1), but there was also significant variability of which residues shifted more among the three repeats (Fig. 4a). Some amide cross peaks which were nearly invisible in CR17 (C2762, C2768) became well resolved upon addition of ApoE(130-149) hinting that slow dynamics in apo CR17 are reduced in the ApoE(130-149)-bound form.

Due to the weak binding and small shifts, three different fitting methods were implemented to calculate  $K_{DS}$  from these titrations, giving remarkably similar results for most cases (Table 1). These calculations revealed that CR17 had the highest affinity for ApoE(130-149) in both isolated ( $930 \mu\text{M}$ ) and in the context of CR16-18 ( $650 \mu\text{M}$ ), similar to values for LA4 (1.1mM) from the LDLR (Table 1, Fig. 4b). CR18 had a weaker affinity (1.6mM) both alone and in the context of CR16-18. CR16 had a very weak affinity as an isolated repeat (3.2mM) but a strong affinity in the context of CR16-18 ( $733 \mu\text{M}$ ). LA5 and especially LA3 showed a very weak affinity (3.9mM and  $>5\text{mM}$  respectively) for ApoE(130-149).

To ensure the observed affinity was purely the result of the interaction with ApoE(130-149), CR17 was also titrated with two variants of ApoE; Ub-ApoE(130-149)(K143/146A) and Ub-

ApoE(130-140). These titrations showed that the double mutation of the critical lysines, K143 and K146 to alanines significantly weakened binding (3.5mM), and truncation of the last nine residues (ApoE(130-140)) nearly abolished it (>5mM). Similarly, mutation of D2778 in CR17 (D2778A), that has been shown to be important for RAP binding, decreased the affinity for ApoE(130-149) significantly (3.5mM) (14).

The results from titrations of the LRP CRs with ApoE(130-149) indicated that individual CRs could each bind ApoE(130-149). To see whether RAP, might elicit similar chemical shift perturbations in the CRs, we titrated the individual CRs with RAPD3. Although two CRs are known to be required for high affinity binding of RAPD3 (14), strong chemical shift perturbations were observed with single CRs (Supp. Fig. 4). In CR17 and LA4 the largest perturbation was a downfield <sup>1</sup>H shift for the indole of W2773 and W144, exactly as seen with ApoE(130-149). The overall pattern of shifted residues was similar to that from ApoE(130-149) binding, with notable differences in the direction of shifts for R2772, W2773, and D2778. The C2781 amide also showed a large perturbation, and the cross peaks for C2762, C2768, which were weak in CR17 became stronger upon ApoE(130-149) binding but disappeared upon RAPD3 binding. Cross peaks in CR18 showed both fast and slow exchange kinetics when perturbed by RAPD3 binding. C2806, N2808, D2821, and D2823, showed the largest perturbations with fast exchange, of which D2823 shifted in the same direction as upon ApoE(130-149) binding (Supp. Figs. 2 and 4). Cross peaks for D2800, D2812, K2814, and F2816 could not be followed due to the slow kinetics of exchange. The fast exchanging chemical shift perturbations were fit to titration curves in the same manner as was done for ApoE (Table 1). Each of the individual CRs bound RAPD3 roughly ten-fold tighter than ApoE(130-149). CR17, CR18 and LA4 had the strongest affinities (35μM, 58μM and 49μM respectively) (Table 1, Fig. 4c). LA3 and LA5 had a much weaker affinities (490μM and 670μM), and the mutation of the critical Asp in CR17, (D2778A) again showed a drastic decrease in  $K_D$  for RAPD3 (720μM).

### Binding to ApoE(1-191)•DMPC

To examine the interaction with the full receptor binding site of lipid-complexed ApoE, Flag-tagged LA3-5 and CR16-18 were used for pulldown assays with ApoE(1-191)•DMPC. As expected, both constructs could interact with GST-RAP in a calcium dependent manner (41), but only LA3-5 showed binding to ApoE(1-191)•DMPC. This was a surprising result considering that CR16-18 bound ApoE(130-149) with similar properties and was discovered by sequence similarity to LA3-5. To test whether multiple copies of a CR with high ApoE(130-149) affinity could interact with lipid complexed ApoE, a triple CR17 (CR17<sup>3</sup>) was constructed. Despite a strong interaction with ApoE(130-149) and GST-RAP, CR17<sup>3</sup> showed no interaction with ApoE(1-191)•DMPC (Fig. 5, 6).

D149 in LA4, D2778 in CR17 and D2821 in CR18 (all equivalent to D30 in the consensus) showed chemical shift perturbation upon RAPD3 binding in NMR titrations, and mutation of this residue in CR17 disrupted binding of ApoE(130-149) and RAPD3 (see above). We mutated each of these to Ala in LA3-5 and CR16-18 to test for effects on ApoE(1-191)•DMPC binding. Mutation of D149A(D30A) in LA4 weakened binding to ApoE(130-149) and GST-RAP, and completely abolished ApoE(1-191)•DMPC binding (Fig. 5 and 6). Similarly, alanine mutation of the critical D2778 and D2821(both D30) in CR17 and CR18 dramatically weakened GST-RAP binding and abolished ApoE(130-149) binding. Just like wild-type, this double-mutant also did not bind ApoE(1-191)•DMPC.

LA5, which bound ApoE(130-149) weakly, has a Gly at position 30 instead of an Asp. To test the importance of this site further, we mutated G198D(G30D) and P199A(P31A) in LA5 to introduce this missing Asp. Surprisingly this substitution in LA5 dramatically enhanced both ApoE(130-149) and calcium dependent ApoE(1-191)•DMPC binding (Fig. 5 and 6). This

mutation also increased binding to the scrambled peptide indicating an increase in non-specific binding of the ApoE(130-149). Thus, D30 is an important residue for ApoE binding, but there must be other key determinants for binding ApoE(1-191)•DMPC that are missing from CR16-18.

To investigate other properties of LA3-5 that promoted interaction with ApoE, sequences of LA45 from several species were aligned, along with the corresponding repeats VLA56 in VLDLR (Fig. 7a). Beyond residues conserved in all CR/LA repeats, LA4 and VLA5 showed complete conservation of a Trp at position 25 and an acidic residue at position 30 (cf. Fig. 1). These residues, however, are also present in CR17 and thus, no uniquely conserved residues were found in LA4/VLA5 that might account for enhanced binding of ApoE(1-191)•DMPC. However, alignments of LA5 and VLA6 showed an additional set of highly conserved residues: E11, S17, E19, H22, W25, and K34 that were not all present in any of the CRs in LRP. While E11, S17 and W25 are quite common among all CRs in several receptors, E19 and H22 along with K34 are very rare. Previously published alignments of LA5s from various species also found H22, W25 and K34 (52), and residues at positions 11 and 19 were implicated in the interface of LA3 of VLDL-R with rhinovirus capsid (53).

To probe the importance of these residues, mutations E180A(E11A), E187A(E19A), H190A(H22A) in LA5 were made in LA3-5. HPLC analysis of the refolded mutants showed that E180A(E11A) and E187A(E19A) mutants, did not refold to a single isoform. Further mutants E187Q(E19Q) and E187A(E19A)/K202L(K34L) also were not able to properly refold. Mutation of H190A(H22A) in LA5 had little effect on RAP binding, but weakened overall ApoE(1-191)•DMPC binding (Fig. 6). Similar to the G198D/P199A mutant, the H190A mutation also increased binding to the scrambled peptide indicating an increase in non-specific binding of the ApoE(130-149) (Fig. 5). Since we had no way of testing the importance of E187 (E19) because these mutations did not refold correctly, we instead attempted to substitute the entire beta strand (residues 186-193 of LA5) into CR18 to create a possible gain-of-function CR18 variant; CR18( $\beta$ 2swap). This swap introduced three substitutions of residues we hypothesized are critical for binding ApoE(1-191)•DMPC; Q19E, and K22H, and F25W. To test the importance of lysine at position 34 we also introduced the A2825K(A34K) mutation into the CR16-18( $\beta$ 2swap) variant. Fortunately both CR16-18( $\beta$ 2swap) variants refolded correctly, and could interact with GST-RAP (Fig. 6). These mutants bound more strongly to ApoE(130-149) and more importantly, unlike wild type, could now interact with ApoE(1-191)•DMPC in a calcium dependent manner (Fig. 5,6). All binding data for the various constructs are summarized in Table 2. The CR16-18( $\beta$ 2swap) showed a specific interaction for ApoE(1-191)•DMPC that was inhibited by both EDTA and GST-RAP just like LA3-5 (Fig. 6c). As a single repeat the CR18( $\beta$ 2swap) construct was also able to interact with Ub-ApoE(130-149) with a significantly higher affinity than WT (745 +/- 180 vs. 1588 +/- 338 $\mu$ M).

## Discussion

### Overall sequence similarity does not reveal ApoE binding capability

Much is known about the context in which ApoE binds LDLR receptor family members, but little is known about which specific regions within the receptors bind to which specific sequences in ApoE. The dearth of information is partly due to the inability to prepare monomeric binding active ApoE so that single specific binding events can be examined. We used sequence alignments to identify regions within the sLRPs of LRP potentially capable of binding ApoE based on sequence similarity to an ApoE binding region (LA3-5) of LDLR. We had previously shown that residues 130-149, a critical receptor binding region in ApoE, could interact with each sLRP of LRP (32). Despite their similarity to LA3-5, neither CR3-5 from sLRP2 nor CR25-27 from sLRP4 showed significant affinity for ApoE(130-149). In contrast, CR16-18 in sLRP3 was able to recapitulate the full binding affinity for this portion of ApoE



that was observed for full sLRP3. It remains possible that other effects such as glycosylation, misfolding, or proteolytic clipping may have prevented CR3-5 and CR25-27 from binding. Regardless of this caveat, CR16-18 remained the focus of the rest of the work presented here.

### Importance of the ApoE(130-149) receptor binding region and resemblance to RAP

CR16-18 was prepared in the same manner as LA3-5 and proper refolding was verified by calcium binding analyses and overlays of HSQC spectra with the individual repeats (Fig. 3). Both affinity pulldowns and SPR confirmed that the refolded CR16-18 could interact with ApoE(130-149) in a calcium dependent manner and the interaction was inhibited by RAP and heparin in agreement with previous reports of other similar interactions (32,41).

Although subtle differences in which residues shifted in NMR titration of each CR with ApoE (130-149), the largest changes were always seen for residues between the third and fifth cysteines (Fig. 4a). Comparisons of ApoE(130-149) and RAPD3 titrations with single repeats indicated that the interfaces, to some extent, were similar. For both ligands the largest perturbation in CR17 and LA4 was seen in the indole of a semi-conserved tryptophan at position 25 (cf Fig. 1, Supp Fig. 2, 4). In addition the amide of the W25 and several nearby residues were highly shifted with both RAPD3 and ApoE(130-149) indicating that this region is involved in both interfaces.

Although ApoE(130-149) NMR titrations resulted in high uncertainty for the measured  $K_D$ , the multiple calculation methods ensured that overall trends were consistent (Table 1). The data indicate that each CR can bind Ub-ApoE(130-149) with a relatively weak affinity (high  $\mu$ M to low mM). CR17 had the strongest affinity for both ApoE(130-149) and RAPD3, with  $K_D$ s similar to those seen with LA4. Both of these repeats have a Trp at position 25 and an Asp at position 30 (Fig. 8c). NMR titrations and pulldown assays agree that mutation of D30 ruins the interaction with RAP in agreement with previous studies (14). We now show that this particular Asp is also critical for the binding of ApoE(1-191)•DMPC. Both CR18 and LA3 have this critical Asp at position 30 but lack a Trp at position 25, which can explain their weaker affinity for ApoE(130-149). However, CR18 retains affinity for RAPD3 whereas LA3 has a very weak affinity for RAPD3, indicating that the RAP interaction is also dependent on residues beyond this W25/D30 pair.

In the crystal structure of RAPD3 bound to LA34, in which W144(W25) and D149(D30) in LA4 are at the center of the interface making contacts with lysines of RAP (54). CR17 probably binds RAPD3 with the same interface as seen in the crystal structure with LA4, as the largest perturbations W2778, R2777, C2781, and D2778 are at this interface. Two lysines of RAP are buried in this interface, and it is thought that lysines 143 and 146 of ApoE are similarly involved in receptor binding (28,54,55). Consistent with this, our ApoE(130-149; K143/146A) double mutant showed significantly decreased affinity for CR17.

Unlike CR17 and CR18, CR16 had a much stronger affinity for ApoE(130-149) in the context of CR16-18 (730 $\mu$ M vs. 3.2mM). This could be an effect of structural and dynamic perturbations from the presence of the neighboring CR17. The similar binding affinities of CR16 and CR17 when in the context of CR16-18 may lead to the speculation that only one ApoE(130-149) is binding both repeats. We think this is unlikely because the chemical shift changes observed in the single domains are identical to those observed when the domains are in the context of CR16-18. A similar enhancement was observed for LA45 binding ApoE which may also be a result of inter-domain crosstalk (Guttman et al., submitted).

### Avidity may account for much of the observed binding

Initial SPR experiments with CR16-18 gave  $K_D$ s in the high nM range, whereas NMR perturbation experiments with ubiquitin-fused ApoE(130-149) showed each repeat within CR16-18 binding ApoE with only high  $\mu$ M affinity. Since these affinities were not much higher than was observed for each individual repeat, the high affinity measured for CR16-18 by SPR and pulldown assay was therefore likely caused by an avidity effect in which multiple repeats simultaneously engage immobilized ApoE(130-149) molecules. This also explains the significant decrease in affinity observed upon removal of any of the three CRs.

It has previously been proposed that avidity effects, in which several interactions occur simultaneously with many copies of ApoE on LDL particle surfaces, govern the binding to the receptor (56). Modified ApoE•DMPC particles which contain only a single copy of active ApoE showed a 26 fold decrease in affinity for receptors compared to those with four active copies (57). Native lipoprotein particles can contain many copies of ApoE, so it is possible that much like in our ApoE(130-149) studies, multiple weak interactions would account for tight binding (Fig. 8a). A similar avidity effect was also seen for the interaction between VLDLR repeats and human rhinovirus capsid (53). The observation that incorporation of ApoE (129-169) into lipoprotein particles enhances receptor-mediated particle uptake (30) can also be explained by this avidity mechanism.

### A distinct binding site on lipid-bound ApoE for LA5

Despite the interactions that were seen with ApoE(130-149), CR16-18 failed to show any interaction with ApoE(1-191)•DMPC (Fig. 6). CR17<sup>3</sup> which has an even higher affinity for ApoE(130-149) was also unable to interact with lipid bound ApoE(1-191). Since all the constructs were correctly folded as assessed by HPLC and GST-RAP binding (Fig. 6), these results strongly suggest that ApoE(1-191)•DMPC interactions involve additional features within the CR repeats beyond those required for binding ApoE(130-149). Alignments of LA45 and VLA56, thought to be the crucial repeats for ApoE binding (41,43), show high conservation of the critical W25/D30 pair in LA4 and VLA5. However LA5, which is the most critical repeat for  $\beta$ -VLDL binding (42), does not have this Asp. Introduction of an Asp at position 30 in LA5 unexpectedly improved the binding to ApoE•DMPC (Fig. 6). This Asp in LA5 is not required for ApoE•DMPC binding but additional acidic residues may be enhancing electrostatic interactions with ApoE, which also explain the increased binding to both ApoE(130-149) and the scrambled ApoE peptide.

Since ApoE undergoes structural rearrangement upon incorporation into lipid particles (34, 35,37) we speculated that this form of ApoE has an additional binding site which is recognized by LA5. Examination of conserved residues in LA5 and VLA6 showed a different set of conserved residues (Fig. 7a). E187(E19) and H190(H22) were particularly interesting as they are very rare among these repeats but completely conserved in LA5 and VLA6 among several species. In addition to being involved in the intra-molecular interface with LDLR's  $\beta$ -propeller domain at endosomal pH (52) (Fig. 7c), pulldown assays with the H190A mutant showed that the conserved H190(H22) in LA5 is also important for ApoE(1-191)•DMPC binding (Fig. 6). In contrast, E187 is not positioned near the interface of LA5 with the  $\beta$ -propeller domain (Fig. 7c). Mutation of E180(E11) and E187(E19) yielded misfolded protein, indicating that these residues are necessary for proper refolding of LA5. Previous Ala saturation mutagenesis also implicated H190(H22) in ApoE binding and could not test E187(E19) due to similar refolding problems (58).

When E187 (E19) along with H190 (H22) was introduced into CR18, it produced a CR16-18 variant ( $\beta$ 2-swap) that could bind to ApoE(1-191)•DMPC in a calcium dependent manner (Fig. 6a). Lysine 202, which is semi-conserved in LA5/VLA6, and is involved with the interaction

with the  $\beta$ -propeller domain (52), was also introduced into this CR16-18 construct but had little effect on ApoE binding. Since CR18 has a native E11 its role was not tested, thus it is still unclear whether it is critical. This  $\beta$ 2-swap mutation also enhanced the interaction with ApoE (130-149), as seen both by pulldown assays and NMR titrations, which can be explained by the substitution of the native Phe at position 25 with a Trp, forming the critical W25/D30 pair. The addition of this tryptophan cannot solely account for the increase in ApoE(1-191)•DMPC binding, as CR17<sup>3</sup> containing three copies with the critical Asp/Trp pair showed no binding to this form of ApoE (Table 2).

Taken together, these results suggest that two distinct binding events are occurring between ApoE and the LA45 repeats of LDLR (Fig. 8b). The first repeat (LA4) containing the W25/D30 pair, likely interacts with the 140–150 site, and the second repeat (LA5) containing an E19, H22, W25 and possibly E11, recognizes the second site that is revealed when ApoE associates with lipid particles. It is possible that helical extension of the region following residue 160 of ApoE forms this second site (40), and that it involves the critical R172 (39).

### Comparison of LDLR and LRP

In the full native interaction between LDL particles and receptors, high affinity recognition could stem from both avidity effects and lipid-induced reorganization of ApoE. Such a model might explain the observation that LDLR can clear several classes of ApoE containing lipoproteins but LRP has only been shown to internalize ApoE enriched  $\beta$ -VLDLs (4). LRP lacks a repeat with the critical residues in LA5, but has many repeats with the critical W25/D30 pair. Although the three-repeat construct used here was not sufficient, the larger number of repeats in the full sLRPs might form enough weak interactions to bind lipoprotein particles rich in ApoE (Fig. 8a). In contrast, LDLR has both types of critical repeats necessary for high affinity binding, explaining why LA45 alone showed high affinity to ApoE(1-191)•DMPC (41). The observation that sLRPs 2 and 4 of LRP had higher affinities for  $\beta$ -VLDL (16) is also in agreement with this model as these two sLRPs contain more repeats with the critical W25/D30 pair (7/8 in SLRP2, 7/11 in SLRP4, only 3/10 in SLRP3). Thus lipoprotein uptake and cholesterol homeostasis may be regulated by both avidity and specific binding interactions.

### Supplementary Material

Refer to Web version on PubMed Central for supplementary material.

### Acknowledgments

We thank Peter J. Domaille, Ph. D. and Sangwon Lee, Ph. D. for help in setting up NMR experiments. We also thank Stephen C. Blacklow, M.D., Ph. D. for ApoE constructs. This research was supported by NIH grant AG025343.

This work was supported by NIH grant AG025343

### Abbreviations

ApoE	Apolipoprotein E
CR	complement-type repeat
LA	ligand binding repeat of LRP
DMPC	dimyristoyl-phosphatidylcholine
EDTA	ethylenediaminetetraacetic acid
GST-RAP	Glutathione S-transferase fused receptor associated protein
HMW	high molecular weight

HPLC	high performance liquid chromatography
HSQC	heteronuclear single quantum coherence
LA	Ligand binding repeat of LDLR
LDLR	Low density lipoprotein receptor
LRP LDLR	related protein
PCR	polymerase chain reaction
sLRP	ligand binding cluster of LRP
VLA	ligand binding repeat of VLDLR
VLDLR	Very low density lipoprotein receptor

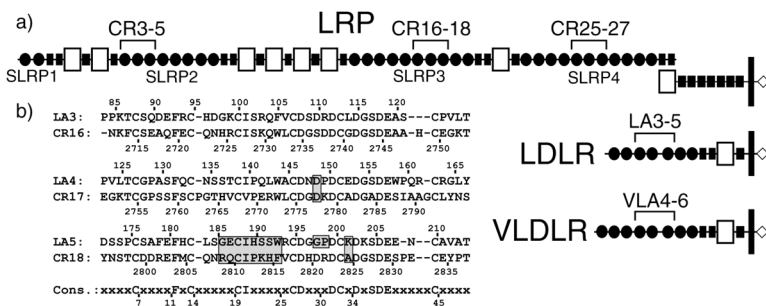
## References

1. Blacklow SC. Versatility in ligand recognition by LDL receptor family proteins: advances and frontiers. *Curr Opin Struct Biol* 2007;17:419–426. [PubMed: 17870468]
2. Brown MS, Goldstein JL. A receptor-mediated pathway for cholesterol homeostasis. *Science* 1986;232:34–47. [PubMed: 3513311]
3. Hui DY, Innerarity TL, Mahley RW. Defective hepatic lipoprotein receptor binding of B-very low density lipoproteins from type 111 hyperlipoproteinemic patients: importance of apolipoprotein E. *J Biol Chem* 1984;259.
4. Kowal RC, Herz J, Goldstein JL, Esser V, Brown MS. Low density receptor-related protein mediates uptake of cholesteryl esters derived from apolipoprotein E-enriched lipoproteins. *Proc Natl Acad Sci USA* 1989;86:5810–5814. [PubMed: 2762297]
5. Hussain MM, Maxfield FR, Más-Oliva J, Tabas I, Ji ZS, Innerarity TL, Mahley RW. Clearance of chylomicron remnants by the low density lipoprotein receptor-related protein/alpha 2-macroglobulin receptor. *J Biol Chem* 1991;266:13936–13940. [PubMed: 1713211]
6. Tacke PJ, Teusink B, Jong MC, Harats D, Havekes LM, van Dijk KW, Hofker MH. LDL receptor deficiency unmasks altered VLDL triglyceride metabolism in VLDL receptor transgenic and knockout mice. *J Lipid Res* 2000;41:2055–2062. [PubMed: 11108739]
7. Takahashi S, Kawarabayasi Y, Nakai T, Sakai J, Yamamoto T. Rabbit very low density lipoprotein receptor: a low density lipoprotein receptor-like protein with distinct ligand specificity. *Proc Natl Acad Sci* 1992;89:9252–9256. [PubMed: 1384047]
8. Herz J, Strickland DK. LRP: A multifunctional scavenger and signaling receptor. *J Clin Invest* 2001;108:779–784. [PubMed: 11560943]
9. Willnow TE, Moehring JM, Inocencio NM, Moehring TJ, Herz J. The low-density-lipoprotein receptor-related protein (LRP) is processed by furin in vivo and in vitro. *Biochem J* 1996;313:71–76. [PubMed: 8546712]
10. Willnow TE, Armstrong SA, Hammer RE, Herz J. Functional expression of low density lipoprotein receptor-related protein is controlled by receptor-associated protein in vivo. *Proc Natl Acad Sci* 1995;92:4537–4541. [PubMed: 7538675]
11. Bu G, Rennke S. Receptor-associated protein is a folding chaperone for low density lipoprotein receptor-related protein. *Journal of Biological Chemistry* 1996;271:22218–22224. [PubMed: 8703036]
12. Herz J, Goldstein JL, Strickland DK, Ho YK, Brown MS. 39-kDa protein modulates binding of ligands to low density lipoprotein receptor-related protein/alpha 2-macroglobulin receptor. *Journal of Biological Chemistry* 1991;266:21232–21238. [PubMed: 1718973]
13. Andersen OM, Schwarz FP, Eisenstein E, Jacobsen C, Moestrup SK, Etzerodt M, Thøgersen HC. Dominant thermodynamic role of the third independent receptor binding site in the receptor-associated protein RAP. *Biochem J* 2001;40:15408–15417.

14. Andersen OM, Christensen LL, Christensen PA, Sørensen ES, Jacobsen C, Moestrup SK, Etzerodt M, Thøgersen HC. Identification of the minimal functional unit in the low density lipoprotein receptor-related protein for binding the receptor-associated protein (RAP). A conserved acidic residue in the complement-type repeats is important for recognition of RAP. *J Biol Chem* 2000;275:21017–21024. [PubMed: 10747921]
15. Willnow TE, Orth K, Herz J. Molecular dissection of ligand binding sites on the low density lipoprotein receptor-related protein. *Journal of Biological Chemistry* 1994;269:15827–15832. [PubMed: 7515061]
16. Neels JG, van den Berg BMM, Lookene A, Olivecrona G, Pannekoek H, van Zonneveld AJ. The second and fourth cluster of class A cysteine-rich repeats of the low density lipoprotein receptor-related protein share ligand binding properties. *J Biol Chem* 1999;274:31305–31311. [PubMed: 10531329]
17. Horn IR, van den Berg BM, van der Meijden PZ, Pannekoek H, van Zonneveld AJ. Molecular analysis of ligand binding to the second cluster of complement-type repeats of the low density lipoprotein receptor-related protein. Evidence for an allosteric component in receptor-associated protein-mediated inhibition of ligand binding. *Journal of Biological Chemistry* 1997;272:13608–13613. [PubMed: 9153209]
18. Croy JE, Shin WD, Knauer MF, Knauer DJ, Komives EA. All three LDL receptor homology regions of the LDL receptor-related protein (LRP) bind multiple ligands. *Biochemistry* 2003;42:13049–13057. [PubMed: 14596620]
19. Beisiegel U, Weber W, Ihrke G, Herz J, Stanley KK. The LDL-receptor-related protein, LRP, is an apolipoprotein E-binding protein. *Nature* 1989;341:162–164. [PubMed: 2779654]
20. Mokuno H, Yamada N, Shimano H, Ishibashi S, Mori N, Takahashi K, Oka T, Yoon TH, Takaku F. The enhanced cellular uptake of very-low-density lipoprotein enriched in apolipoprotein E. *Biochim Biophys Acta* 1991;1082:63–70. [PubMed: 1849015]
21. Blacklow SC, Kim PS. Protein folding and calcium binding defects arising from familial hypercholesterolemia mutations of the LDL receptor. *Nat Struct Biol* 1996;3:758–762.
22. Rudenko G, Deisenhofer J. The low-density lipoprotein receptor: ligands, debates and lore. *Curr Opin Struct Biol* 2003;13:683–689. [PubMed: 14675545]
23. Huang W, Dolmer K, Gettins PG. NMR solution structure of complement-like repeat CR8 from the low density lipoprotein receptor-related protein. *J Biol Chem* 1999;274:14130–14136. [PubMed: 10318830]
24. Rall SCJ, Weisgraber KH, Innerarity TL, Mahley RW. Structural basis for receptor binding heterogeneity of apolipoprotein E from type III hyperlipoproteinemic subjects. *Proc Natl Acad Sci* 1982;79:4696–4700. [PubMed: 6289314]
25. Innerarity TL, Friedlander EJ, Rall SCJ, Weisgraber KH, Mahley RW. The Receptor Binding Domain of Human Apolipoprotein E. Binding Of Apolipoprotein E fragments. *J Biol Chem* 1983;258:12341–12347. [PubMed: 6313652]
26. Weisgraber KL, Innerarity TL, Harder KJ, Mahley RW, Milne RW, Marcel YL, Sparrow JT. The Receptor Binding Domain Of Human Apolipoprotein E. *J Biol Chem* 1983;258:12348–12354. [PubMed: 6313653]
27. Lalazar A, Weisgraber KH, Rall SCJ, Gilad H, Innerarity TL, Levanon AZ, Boyles JK, Amit B, Gorecki M, Mahley RW, Vogel T. Site-specific Mutagenesis of human apolipoprotein E. Receptor binding activity of variants with single amino acids substitutions. *J Biol Chem* 1988;263:3542–3545. [PubMed: 2831187]
28. Zaiou M, Arnold KS, Newhouse YM, Innerarity TL, Weisgraber KH, Segall ML, Phillips MC, Lund-Katz S. Apolipoprotein E<sub>3</sub>-low density lipoprotein receptor interaction. Influences of basic residue and amphipathic alpha-helix organization in the ligand. *J Lipid Res* 2000;41:1087–1095. [PubMed: 10884290]
29. Kiss RS, Weers PM, Narayanaswami V, Cohen J, Kay CM, Ryan RO. Structure-guided protein engineering modulates helix bundle exchangeable apolipoprotein properties. *J Biol Chem* 2003;278:21952–21959. [PubMed: 12684504]

30. Mims MP, Darnule AT, Tovar RW, Pownall HJ, Sparrow DA, Sparrow JT, Via DP, Smith LC. A nonexchangeable apolipoprotein E peptide that mediates binding to the low density lipoprotein receptor. *J Biol Chem* 1994;269:20539–20547. [PubMed: 8051153]
31. Datta G, Garber DW, Chung BH, Chaddha M, Dashti N, Bradley WA, Gianturco SH, Anantharamaiah GM. Cationic domain 141–150 of apoE covalently linked to a class A amphipathic helix enhances atherogenic lipoprotein metabolism in vitro and in vivo. *J Lipid Res* 2001;42:959–966. [PubMed: 11369804]
32. Croy JE, Brandon T, Komives EA. Two apolipoprotein E mimetic peptides, apoE(130-149) and apoE(141-155)<sub>2</sub>, bind to LRP1. *Biochemistry* 2004;43:7328–7335. [PubMed: 15182176]
33. Wilson C, Wardell MR, Weisgraber KH, Mahley RW, Agard DA. Three-dimensional structure of the LDL receptor-binding domain of human apolipoprotein E. *Science* 1991;252:1817–1822. [PubMed: 2063194]
34. Fisher CA, Ryan RO. Lipid binding-induced conformational changes in the N-terminal domain of human apolipoprotein E. *J Lipid Res* 1999;40:93–99. [PubMed: 9869654]
35. Peters-Libeu CA, Newhouse Y, Hatters DM, Weisgraber KH. Model of biologically active apolipoprotein E bound to dipalmitoylphosphatidylcholine. *J Biol Chem* 2006;281:1073–1079. [PubMed: 16278220]
36. Peters-Libeu CA, Newhouse Y, Hall SC, Witkowska HE, Weisgraber KH. Apolipoprotein E. dipalmitoylphosphatidylcholine particles are ellipsoidal in solution. *J Lipid Res* 2007;48:1035–1044. [PubMed: 17308333]
37. Lund-Katz S, Zaiou M, Wehrli S, Dhanasekaran P, Baldwin F, Weisgraber KH, Phillips MC. Effects of lipid interaction on the lysine microenvironments in apolipoprotein E. *J Biol Chem* 2000;275:34459–34464. [PubMed: 10921925]
38. Lalazar A, Mahley RW. Human apolipoprotein E. Receptor binding activity of truncated variants with carboxyl-terminal deletions. *J Biol Chem* 1989;264:8447–8450. [PubMed: 2542277]
39. Morrow JA, Arnold KS, Dong J, Balesta ME, Innerarity TL. Effect of Arginine 172 on the Binding of Apolipoprotein E to the Low Density Lipoprotein Receptor. *J Biol Chem* 2000;275:2576–2580. [PubMed: 10644716]
40. Gupta V, Narayanaswami V, Budamagunta MS, Yamamoto T, Voss JC, Ryan RO. Lipid-induced extension of apolipoprotein E helix 4 correlates with low density lipoprotein receptor binding ability. *J Biol Chem* 2006;281:39294–39299. [PubMed: 17079229]
41. Fisher C, Abdul-Aziz D, Blacklow SC. A two-module region of the low-density lipoprotein receptor sufficient for formation of complexes with apolipoprotein E ligands. *Biochem J* 2004;43:1037–1044.
42. Russell DW, Brown MS, Goldstein JL. Different combinations of cysteine-rich repeats mediate binding of low density lipoprotein receptor to two different proteins. *J Biol Chem* 1989;264:21682–21688. [PubMed: 2600087]
43. Ruiz J, Kouivskaia D, Migliorini M, Robinson S, Saenko EL, Gorlatova N, Li D, Lawrence D, Hyman BT, Weisgraber KH, Strickland DK. The apoE isoform binding properties of the VLDL receptor reveal marked differences from LRP and the LDL receptor. *J Lipid Res* 2005;46:1721–1731. [PubMed: 15863833]
44. Nicholas KB, NHB. GeneDoc: a tool for editing and annotating multiple sequence alignments. 1997
45. White CE, Hunter MJ, Meininger DP, White LR, Komives EA. Large-scale expression, purification and characterization of small fragments of thrombomodulin: the roles of the sixth domain and of methionine 388. *Protein Engineering* 1995;8:1177–1187. [PubMed: 8819984]
46. Fass D, Blacklow S, Kim PS, Berger JM. Molecular basis of familial hypercholesterolaemia from structure of LDL receptor module. *Nature* 1997;388:691–693. [PubMed: 9262405]
47. Clackson, T.; Detlef, G.; Jones, P. PCR, a Practical Approach. McPherson, M.; Quirke, P.; Taylor, G., editors. Vol. 202. IRL Press; Oxford: 1991.
48. Jez MJ, Ferrer J, Bowman ME, Dixon RA, Noel JP. Dissection of Malonyl-Coenzyme A Decarboxylation from Polyketide Formation in the Reaction Mechanism of a Plant Polyketide Synthase. *Biochemistry* 2000;39:890–902. [PubMed: 10653632]
49. Hoffman RMB, Li MX, Sykes BD. The Binding of W7, an Inhibitor of Striated Muscle Contraction, to Cardiac Troponin C. *Biochemistry* 2005;44:15750–15759. [PubMed: 16313178]

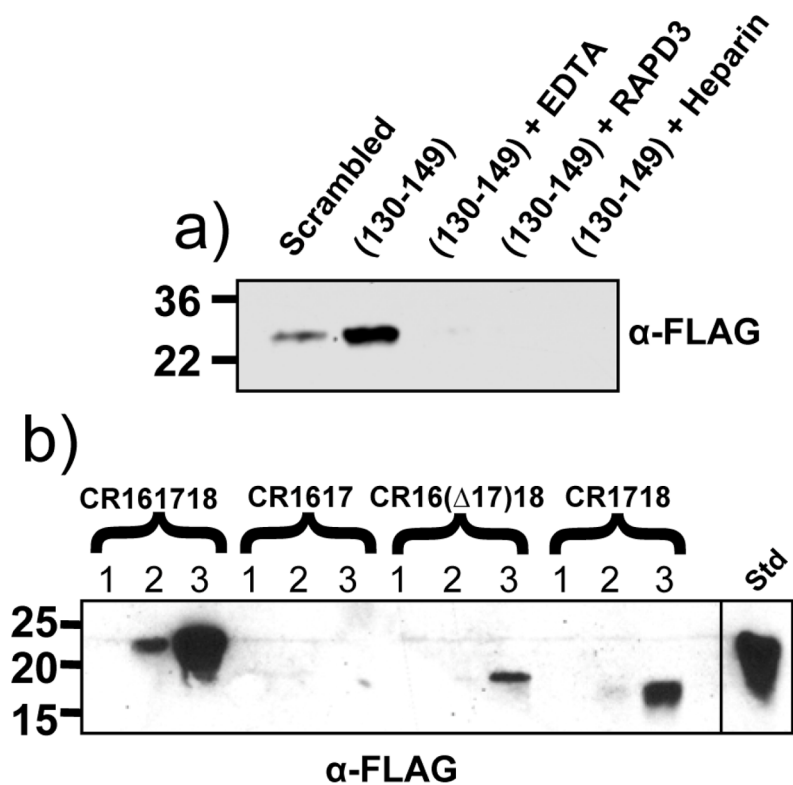
50. Andersen OM, Vorum H, Honoré B, Thøgersen HC. Ca<sup>2+</sup> binding to complement-type repeat domains 5 and 6 from the low-density lipoprotein receptor-related protein. *BMC Biochemistry* 2003;4. [PubMed: 12735798]
51. Simonovic M, Dolmer K, Huang W, Strickland DK, Volz K, Gettins PGW. Calcium Coordination and pH dependence of the calcium affinity of ligand-binding repeat CR7 from the LRP. Comparison with related domains from the LRP and the LDL receptor. *Biochemistry* 2001;40:15127–15134. [PubMed: 11735395]
52. Rudenko G, Henry L, Henderson K, Ichtchenko K, Brown MS, Goldstein JL, Deisenhofer J. Structure of the LDL receptor extracellular domain at endosomal pH. *Science* 2002;298:2353–2358. [PubMed: 12459547]
53. Verdaguer N, Fita I, Reithmayer M, Moser R, Blaas D. X-ray structure of a minor group human rhinovirus bound to a fragment of its cellular receptor protein. *Nat Struct Mol Biol* 2004;11:429–434. [PubMed: 15064754]
54. Fisher C, Beglova N, Blacklow SC. Structure of an LDLR-RAP complex reveals a general mode for ligand recognition by lipoprotein receptors. *Mol Cell* 2006;22:277–283. [PubMed: 16630895]
55. Prévost M, Raussens V. Apolipoprotein E-low density lipoprotein receptor binding: study of protein-protein interaction in rationally selected docked complexes. *Proteins* 2004;55:874–884. [PubMed: 15146486]
56. Mahley RW, Innerarity TL, Rall SC, Weisgraber KH. Plasma lipoproteins: apolipoprotein structure and function. *J Lipid Res* 1984;25:1277–1294. [PubMed: 6099394]
57. Pitas RE, Innerarity TL, Mahley RW. Cell surface receptor binding of phospholipid. protein complexes containing different ratios of receptor-active and -inactive E apoprotein. *J Biol Chem* 1980;255:5454–5460. [PubMed: 7372644]
58. Abdul-Aziz D, Fisher C, Beglova N, Blacklow SC. Folding and binding integrity of variants of a prototype ligand-binding module from the LDL receptor possessing multiple alanine substitutions. *Biochem J* 2005;44:5075–5085.



**Figure 1.**

**a)** Schematic diagram of LRP, LDL, and VLDL showing CR/LA modules (circles), EGF domains (black rectangles),  $\beta$ -propeller domains (clear rectangles), and intracellular domain (diamonds). **b)** Sequence alignment of LA3-5 with CR16-18 with overall consensus for complement repeats (21). Highlighted portions were mutated in this study, including the  $\beta$ 2-swap mutation inserting residues 186-193 of LA5 into CR18 at positions 2809–2816.



**Figure 2.**

**a)** FLAG-tagged CR16-18 was tested for binding to a scrambled ApoE peptide, and ApoE (130-149) (both biotinylated and bound to streptavidin beads) in the presence of EDTA, RAP, and HMW heparin. The bound CR16-18 was visualized by anti-FLAG immunoblotting. **b)** Same affinity assay as a) comparing smaller double repeats from CR16-18 with (1) 2.0  $\mu$ M CR domain and unconjugated beads, (2) 100nM CR domain and immobilized ApoE(130-149), or (3) 2.0  $\mu$ M CR domain and immobilized ApoE(130-149).

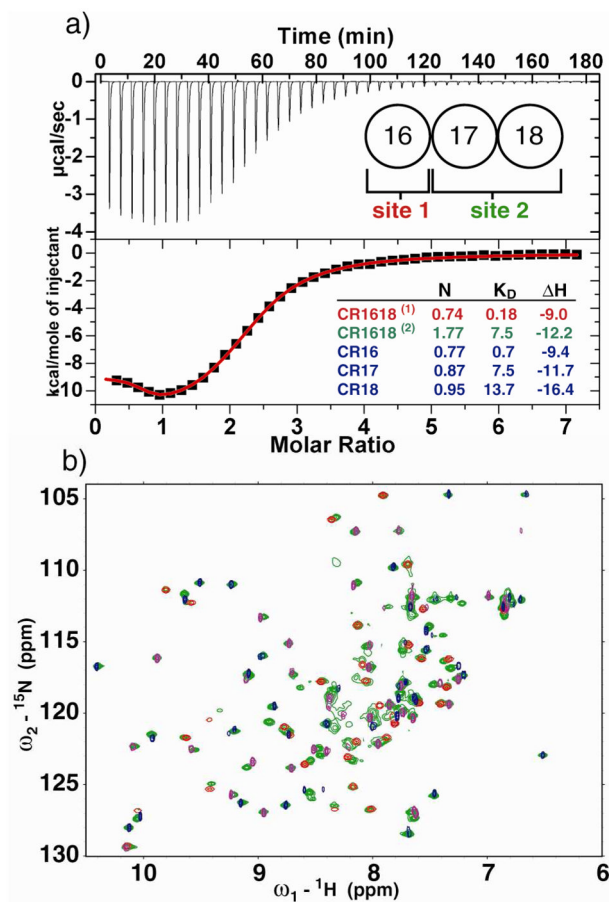


**Figure 3.**  
**a)** Calcium binding isotherm of CR16-18. The inset provides values for the stoichiometry (N), the  $K_D$  ( $\mu\text{M}$ ) and the  $\Delta H$  (kcal/mol) are listed for each isolated CR (blue font) as well as for the fits of site (1) (red font) and (2) (green font) in CR16-18. **b)** NMR HSQC spectral overlays of CR16 (blue), CR17 (red), CR18 (purple), and CR16-18 (green) under identical conditions.

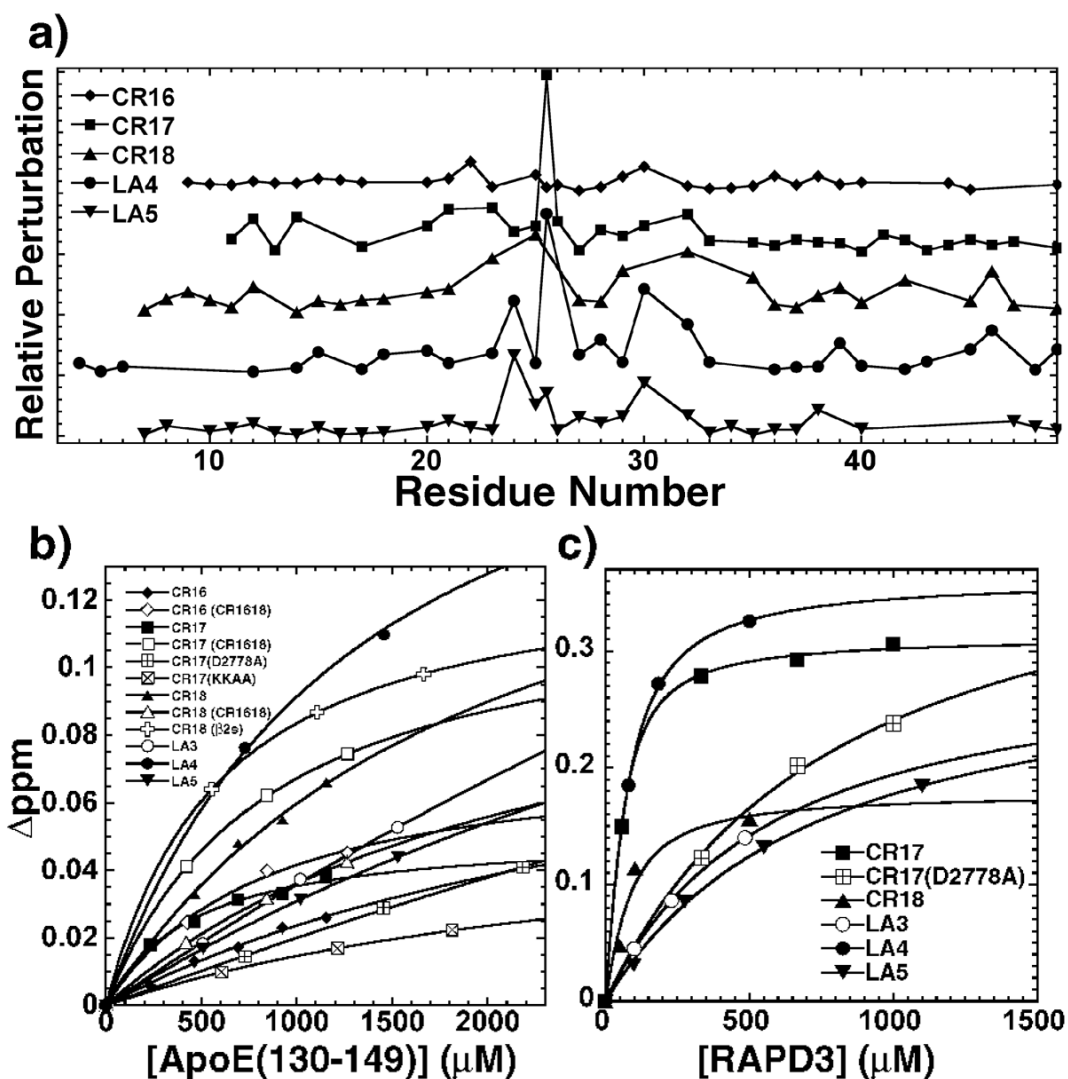


**Figure 4.**

a) Plot of relative amide perturbation for each residue in CR16 ( $\blacklozenge$ ), CR17 ( $\blacksquare$ ), CR18 ( $\blacktriangle$ ), LA4 ( $\bullet$ ), and LA5 ( $\blacktriangledown$ ). CRs are each renumbered for alignments shown in Fig. 1b, and indole sidechains of W25 are plotted at the x-axis value of 25.5. b) NMR titrations plots for Ub-ApoE (130-149) with: CR16 ( $\blacklozenge$ ), CR16 in CR16-18 ( $\blacklozenge$ ), CR17 ( $\blacksquare$ ), CR17 in CR16-18 ( $\square$ ), CR17 (D2778A) ([+]), CR17 with ApoE(130-149) (K143/146A) ([X]), CR18 ( $\blacktriangle$ ), CR18 in CR16-18 ( $\triangle$ ), CR18( $\beta$ 2swap) (+), LA3 ( $\circ$ ), LA4 ( $\bullet$ ), and LA5 ( $\blacktriangledown$ ). c) NMR titrations for Ub-RAPD3 with the same symbols from b). For both plots the largest resolvable amide perturbation was plotted against the ligand concentration.

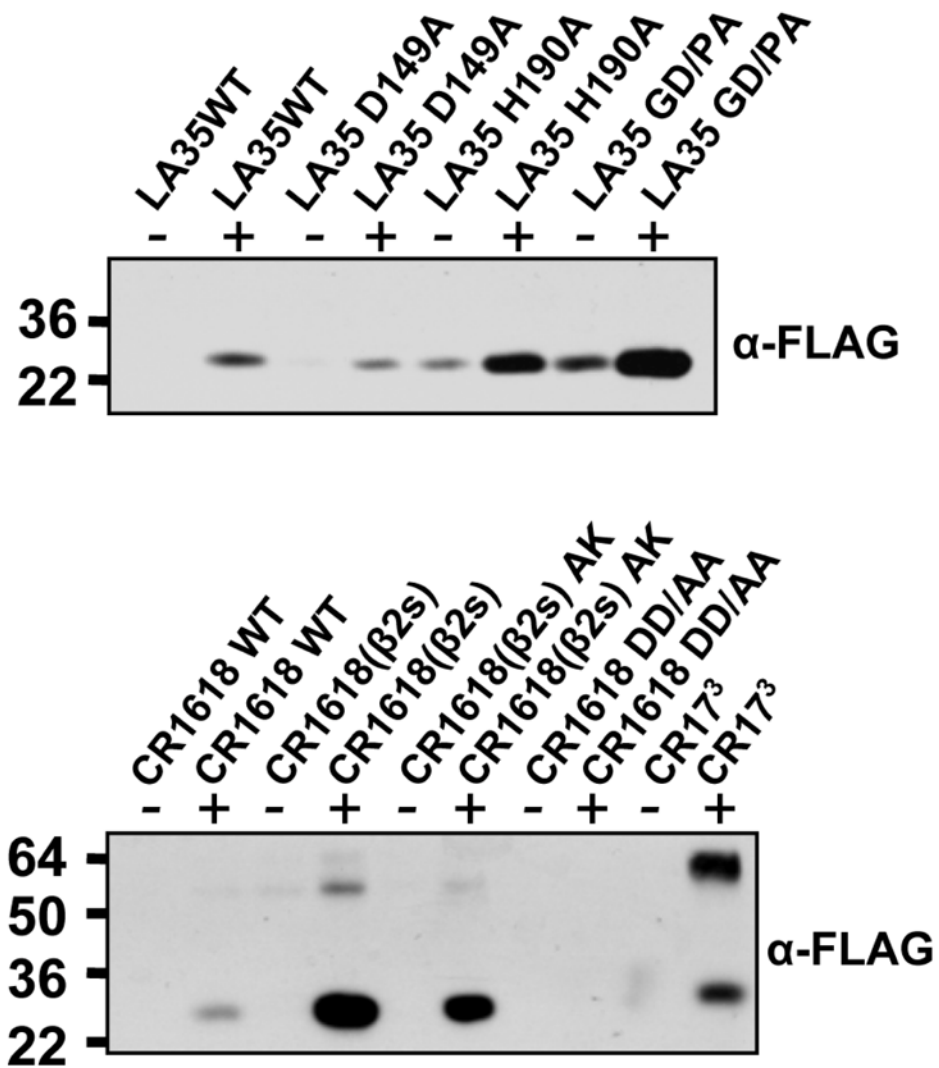


**Figure 5.** Affinity pull-downs of various LA/CR constructs to scrambled peptide (-) or ApoE(130-149) (+), visualized by anti-FLAG immunoblotting. LA35 GD/PA refers to G198D/P199A, CR1618( $\beta$ 2s) refers to the  $\beta$ 2swap mutant, AK is the A2825K mutation in CR18 ( $\beta$ 2swap), and CR1618 DDAA is the D2778A/D2821A double mutant.

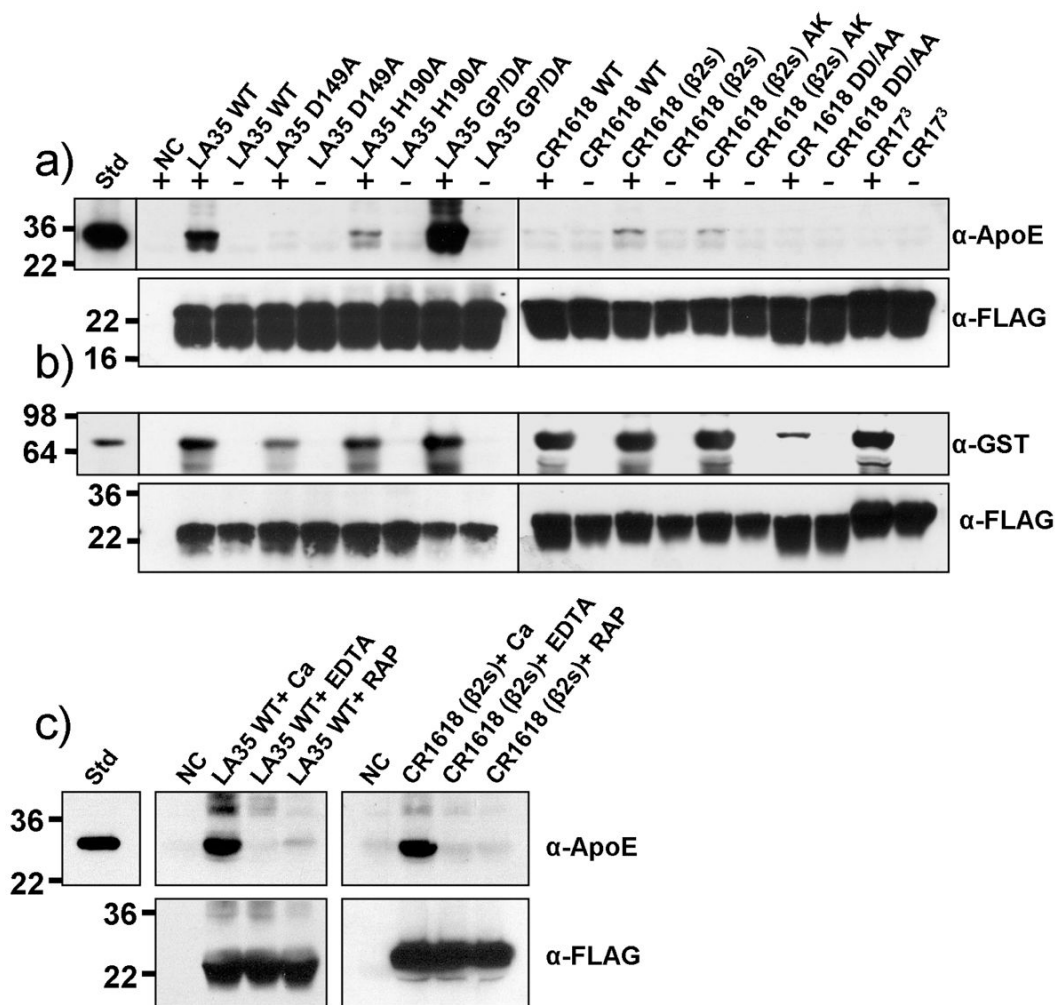


**Figure 6.**

**a)** Various LA/CR constructs and mutants were assayed for binding ApoE(1-191)•DMPC particles in the presence of calcium (+) or EDTA (-). Blots were visualized by  $\alpha$ -ApoE (top) and anti-FLAG (bottom) immunoblotting. **b)** Same CR/LA constructs assayed for GST-RAP binding, visualized by  $\alpha$ -GST (top) and anti-FLAG (bottom) immunoblotting. LA35 GD/PA refers to G198D/P199A, CR1618( $\beta$ 2s) refers to the  $\beta$ 2swap mutant, AK is A2825K mutation in CR18( $\beta$ 2swap), CR1618 DDAA the D2778A/D2821A double mutant. **c)** Binding assays of LA3-5 and CR16-18( $\beta$ 2s) binding ApoE(1-191)•DMPC and inhibition with EDTA, and GST-RAP.

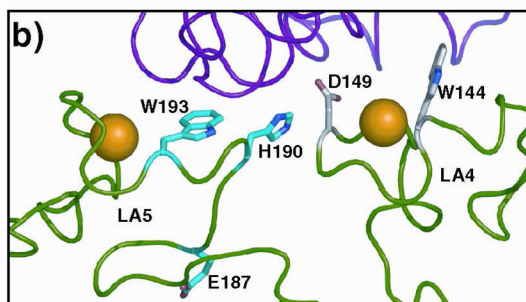
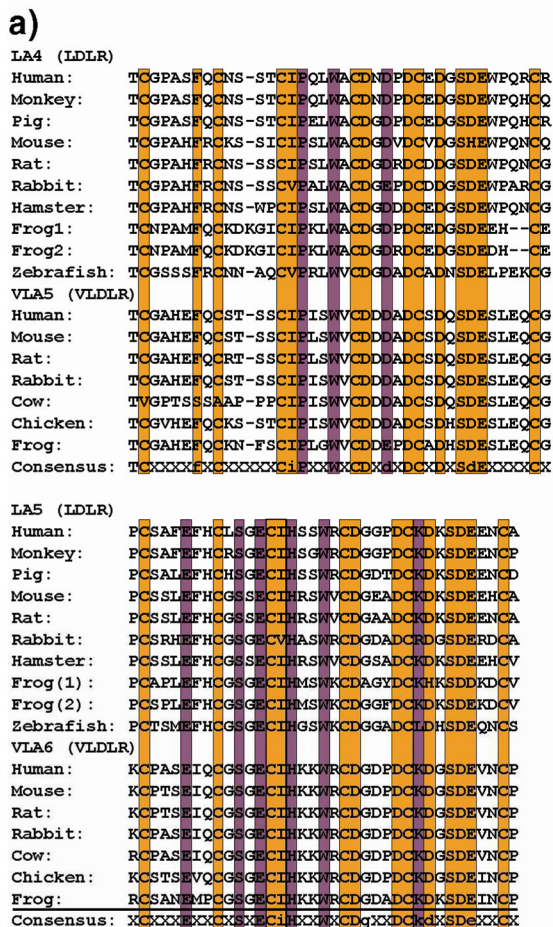


**Figure 7.**

**a)** Sequence alignment of LA4/VLA5 and LA5/VLA6 from various species. Consensus for these specific repeats is listed as completely conserved (upper case) and mostly conserved (lower case). Residues conserved in all complement repeats (yellow) and residues specifically conserved in these repeats (red) are highlighted. **b)** Structure of LA4 (right) and LA5 (left) (from Rudenko et al., 2002; pdb 1N7D) with the  $\beta$ -propeller domain (magenta), showing the specific residues implicated in binding ApoE residues 140-150 (grey) and residues implicated in binding the second site (cyan).

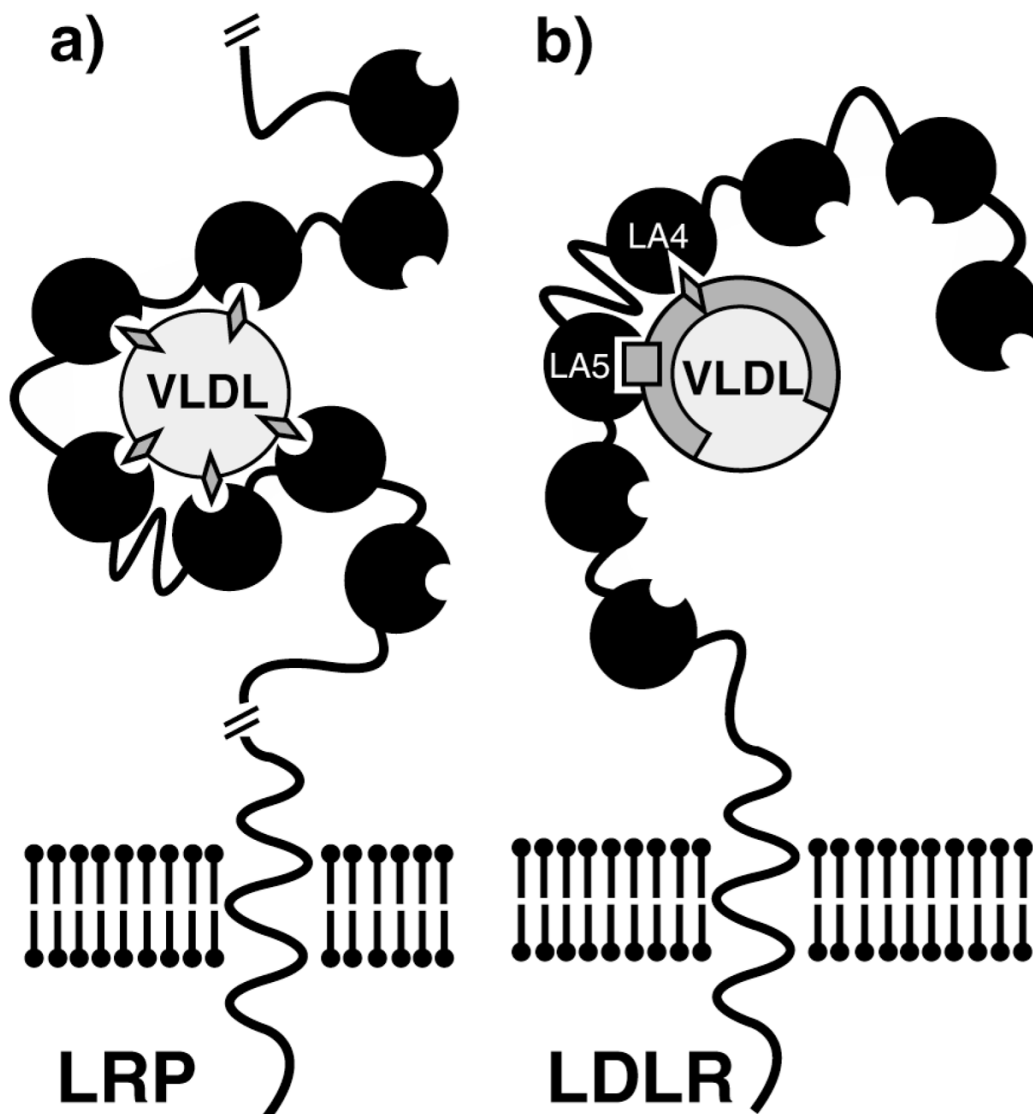


**Figure 8.**

Proposed models of how LRP and LDLR might bind ApoE-containing lipoprotein particles. **a)** Avidity model in which multiple copies of ApoE (grey diamonds) exposed on the particle surface combine many weak interactions with ligand binding repeats (black circles) on LRP into one strong interaction. **b)** The lipoprotein bound form of ApoE present epitopes which are recognized by specific repeats of LDLR. In this case, LA4 is recognizing one epitope on an ApoE molecule (grey diamond), and LA5 is recognizing a different epitope (grey square).

**Table 1**

Binding affinities for various ApoE-LA/CR interactions

	$K_D$ (Global)	$K_D$ (Largest)	$K_D$ (Sum)	$K_D$ (Overall)
Ub-RAPD3 binding				
CR17	$33 \pm 8$	$33 \pm 3$	$40 \pm 6$	$35 \pm 4$
CR17(D2778A)	$710 \pm 62$	$770 \pm 130$	$680 \pm 95$	$720 \pm 46$
CR18	$55 \pm 5$	$57 \pm 30$	$62 \pm 33$	$58 \pm 4$
LA3	$460 \pm 22$	$530 \pm 4$	$480 \pm 40$	$490 \pm 36$
LA4	$52 \pm 5$	$50 \pm 2$	$46 \pm 4$	$49 \pm 3$
LA5	$650 \pm 35$	$700 \pm 70$	$660 \pm 52$	$670 \pm 26$
Ub-ApoE(130-149) binding				
CR16	ND <sup>I</sup>	$3176 \pm 1050$	ND	$3176 \pm ND$
CR17	$1027 \pm 284$	$852 \pm 334$	$912 \pm 205$	$930 \pm 89$
CR17(D2778A)	$3496 \pm 729$	ND	$3545 \pm 250$	$3521 \pm 35$
CR18	$1441 \pm 266$	$1975 \pm 381$	$1349 \pm 163$	$1588 \pm 338$
CR18 ( $\beta$ 2swap)	$756 \pm 61$	$560 \pm 3$	$920 \pm 77$	$745 \pm 180$
CR16(in CR16-18)	$774 \pm 102$	$744 \pm 183$	$681 \pm 67$	$733 \pm 47$
CR17(in CR16-18)	$581 \pm 92$	$757 \pm 7$	$610 \pm 19$	$649 \pm 94$
CR18(in CR16-18)	$1194 \pm 239$	$2249 \pm 220$	$1289 \pm 90$	$1577 \pm 584$
LA3	$8509 \pm 3018$	ND	$9961 \pm 160$	$9235 \pm 1027$
LA4	$1031 \pm 73$	$1197 \pm 106$	$1049 \pm 26$	$1092 \pm 91$
LA5	$3822 \pm 433$	$4189 \pm 538$	$3622 \pm 167$	$3878 \pm 288$
UbApoE (130-149) (K143/146A) binding				
CR17	$3840 \pm 801$	$2761 \pm 361$	$3776 \pm 375$	$3459 \pm 605$
UbApoE (130-140) binding				
CR17	ND	ND	ND	>5mM

<sup>I</sup> ND, certain titrations could not be fit, or yielded  $K_D$  values >5mM with large uncertainty.



**Table 2**

Relative affinities of various CR/LA triple constructs from binding assays with GST-RAP, ApoE(1-191)•DMPC and ApoE(130-149).

	<b>GST-RAP<sup>I</sup></b>	<b>ApoE(1-191)•DMPC</b>	<b>ApoE(130-149)</b>
LA3-5 WT	***	**	**
LA3-5 (D149A)	**	X	*
LA3-5 (H190A)	***	*	***
LA3-5 (GP/DA)	***	***	***
CR16-18 WT	***	X	*
CR16-18 (DDAA)	*	X	X
CR16-18 (β2s)	***	*	***
CR16-18 (β2s/AK)	***	*	***
CR173	***	X	***

<sup>I</sup>Symbols indicate no (X), weak (\*), moderate (\*\*), or strong (\*\*\*) binding.